Published in final edited form as:
J Immunol. 2011 September 15; 187(6): 3121–3132. doi:10.4049/jimmunol.1100378.

FUNCTIONAL GAP JUNCTIONS ACCUMULATE AT THE IMMUNOLOGICAL SYNAPSE AND CONTRIBUTE TO T CELL ACTIVATION

Ariadna Mendoza-Naranjo[1,2,*], **Gerben Bouma**[3], **Cristian Pereda**[1], **Marcos Ramírez**[1], **Kevin F. Webb**[4], **Andrés Tittarelli**[1], **Mercedes N. López**[1], **Alexis M. Kalergis**[5], **Adrian J. Thrasher**[3], **David L. Becker**[4], and **Flavio Salazar-Onfray**[1,*]

[1]Millennium Institute on Immunology and Immunotherapy, Institute of Biomedical Sciences, Faculty of Medicine, University of Chile, 8380453 Santiago Chile, Chile

[2]UCL Cancer Institute, 72 Huntley St, London WC1E 6DD, UK

[3]UCL Institute of Child Health, Molecular Immunology Unit, 30 Guilford St, London WC1N 1EH, UK

[4]Department of Cell and Developmental Biology, UCL, Gower Street, London WC1E 6BT, UK

[5]Millennium Institute on Immunology and Immunotherapy, Department of Molecular Genetic and Microbiology, Pontificia Universidad Católica de Chile, Santiago, Chile

Abstract

Gap junction (GJ) mediate intercellular communication through linked hemichannels from each of two adjacent cells. Using human and mouse models we show that connexin 43 (Cx43), the main GJ protein in the immune system, was recruited to the immunological synapse during T cell priming as both GJs and stand-alone hemichannels. Cx43 accumulation at the synapse was antigen-specific and time-dependent, and required an intact actin cytoskeleton. Fluorescence recovery after photobleaching and Cx43-specific inhibitors were used to prove that intercellular communication between T cells and DCs is bidirectional and specifically mediated by Cx43. Moreover, this intercellular crosstalk contributed to T cell activation as silencing of Cx43 with an antisense or inhibition of GJ docking impaired intracellular Ca^{2+} responses and cytokine release by T cells. These findings identify Cx43 as an important functional component of the immunological synapse and reveal a crucial role for GJs and hemichannels as coordinators of the DC-T cell signaling machinery that regulates T cell activation.

Keywords

calcium signals; Cx43; gap junctions; hemichannels; immunological synapse

Introduction

Initiation of an antigen-specific immune response requires productive engagement of T cell receptors (TCRs) by MHC-peptide complexes (pMHC) on the antigen-presenting cell (APC)

[*]To whom correspondence should be addressed: Disciplinary Program of Immunology, Institute of Biomedical Sciences Faculty of Medicine University of Chile Independencia 1027 Santiago Chile, 8380453 Phone: 44 020 7679 0738; 56 2 978 6345 Fax: 56-2 735 3346 a.mendoza@ucl.ac.uk; flavio.salazar@inmunotro.med.uchile.cl.

Contribution: AMN and FSO designed research; AMN, GB, CP, MR, KFW and AT performed research; DLB, AMK, AJT, and MNL contributed new reagents and analytic tools; AMN, GB and FSO wrote the paper.

Europe PMC Funders Author Manuscripts

(1, 2). This TCR engagement by cognate pMHC results in the formation of a highly organized protein network known as the immunological synapse (IS), which is required for T cell activation and proliferation (3). The mature IS is characterized by the assembly of specific proteins on the T cell and APC membranes into supramolecular activation clusters (SMACs). These structures consist of a centralized accumulation of TCRs and pMHC (cSMAC), surrounded by a peripheral ring (pSMAC) containing the integrin LFA-1 and its receptor ICAM-1 (3, 4).

The IS comprises a multitude of structures, many of which are mediators of intercellular communication (5). However, it is not known whether communication involving gap junction (GJ) channels, one of the most important mechanisms for cellular crosstalk, occurs at the IS assembly site. GJs are clusters of intercellular channels in the plasma membrane that mediate direct intercellular communication between adjacent cells, allowing the passage of soluble molecules including cAMP, Ca^{2+}, ATP, inositol 1,4,5-trisphosphate (Ins(1,4,5)*P*3) and morphogens (6, 7). GJs also mediate electrical and metabolic coupling among cells and tissues, such that signals initiated in one cell can readily propagate to neighbouring cells. In mammals, functional GJs are composed of connexin (Cx) proteins. Six Cxs proteins form a hemichannel (Hchl) inserted into the membrane of one cell, which then docks with a Hchl from an adjacent cell to establish a GJ channel (8, 9).

Cxs and GJ-mediated intercellular communication (GJIC) have been shown to participate in key immunological processes such as immunoglobulin secretion and cytokine production (10), transendothelial migration of leukocytes (11), peptide transfer and cross-presentation in activated monocytes (12), activation of murine dendritic cells (DCs) (13), and regulatory T cell-mediated suppression through the transfer of cAMP (14). Additionally, we have demonstrated that GJ channels can also mediate the transfer of MHC class I-restricted melanoma peptides between human DCs, triggering T cell-specific immune response against melanoma-associated antigens (15). Recently, GJIC have also been shown to participate in DC-mediated induction of IL-2 release and proliferation of murine T cells (16). T cell activation and proliferation result from intercellular communications mediated by multiple surface molecules located at the IS. However, the accumulation of connexins at the IS, the mechanisms involved in their recruitment, and their role in T cells Ca^{2+} signaling and IFN-γ production, has not been elucidated.

In the present study we describe that Cx43, the main GJ protein of the immune system (10, 12, 17-19), accumulates at the IS and mediates bidirectional crosstalk between DCs and T cells in murine and human systems. Moreover, we identify a role for GJs in the regulation of T cell activation.

Materials and methods

Mice

OT-II transgenic mice expressing the ovalbumin $(OVA)_{323-339}$ peptide (ISQAVHAAHAEINEAGR) TCR (H-2b) and wild-type C57BL/6 mice were obtained from Charles River (Kent, United Kingdom). Mice were used at 6 to 12 weeks of age, and all experiments were approved by and performed according to Home Office Animal Welfare Legislation.

Generation of DCs and T cells

This study was approved by the Bioethical Committee of Human Research, Faculty of Medicine, University of Chile. Informed written consents were given and signed by all patients. Leukocytes from stage IV melanoma patients were isolated by density gradient using Ficoll-Hypaque (Axis-Shield, Oslo, Norway). Human DCs were obtained as described

(20). At day 6, DCs were treated overnight with 150 μg/ml of a melanoma cell lysate (MCL), which was obtained as previously described (15), and stimulated with 2 ng/ml TNF-α (US Biological, Swampscott, MA, USA) (MCL-DCs). DCs stimulated with 1 μg/ml LPS plus 2 ng/ml of TNF-α and loaded with 2 μg/ml of $gp100_{209-217}$ peptide (gp100-DCs) were used as negative control. DCs from C57BL/6 mice were cultured from bone marrow cells for 7 days in the presence of GM-CSF (20 ng/ml, Invitrogen, Paisley, UK). For T-cell priming experiments, DCs were maturated overnight with LPS (100 ng/mL; Sigma, Steinheim, Germany) in the presence or absence of ovalbumin (OVA, 100 μg/mL; Sigma).

MT56-4 is a $CD4^+$ T cell line derived from TIL of a melanoma patient, which specifically recognize autologous MCL-DCs and autologous melanoma cells, were isolated and grown as described (15). $CD4^+$ T cells from OT-II transgenic mice were isolated from spleen using magnetic bead separation according to manufacturer's protocol (murine $CD4^+$ T cell isolation kit, Miltenyi Biotec, Bisley, UK).

T cells stimulation and immune fluorescence staining

Dynal M450 beads (Dynal, Lake Success, NY, USA) were coated with 3 μg/ml anti-human CD3 (OKT3) mAb and/or anti-human CD28 mAb (eBioscience, San Diego, CA, USA), as well as with a control (anti-CD8) Ab (BD, Pharmingen, San Jose, CA, USA), according to manufacturer's recommendations. PBLs (2×10^4) from melanoma patients were incubated with 6×10^4 beads for 1 h at 37°C. For some experiments, PBLs were pre-treated or not with 10 μM cytochalasin D (Calbiochem Gibbstown, NJ, USA), 5 nM latrunculin A, 10 μM taxol, or 5 μg/ml nocodazole (last three from Sigma-Aldrich) 30 min before incubation with CD3/CD28-coated beads. In these set of experiments cells were also stained with 5 μg/ml Hoechst 33342 (Invitrogen). Polyclonal anti-Cx43 Ab (21) and/or anti-CD3 mAb, clone HIT3a (BD, Pharmingen) were incubated overnight at 4°C. Samples were stained with Alexa Fluor® 647 goat anti–rabbit (Molecular Probes, Invitrogen, USA) and with TRITC-conjugated rabbit anti-mouse (Sigma, St. Louis, MO, USA) and analyzed by confocal microscopy (LSM 510 META software; Carl Zeiss MicroImaging, Inc., Germany) using a 63x NA 1.4 oil immersion objective (Carl Zeiss). The recruitment of Cx43 to the contact area was quantified as previously described (22). Cells displaying more than 70% of Cx43 staining in the quadrant contacting the bead were scored as positive. One hundred T cell-bead conjugates were analyzed on ~ 25 fields in at least 3 experiments. Two independent investigators evaluated the data.

OVA-DCs or LPS-DCs (1×10^5) were co-incubated for different time periods (15, 30, 45, 60 and 120 min) with 3×10^5 OT-II $CD4^+$ T cells. We allowed the conjugates to adhere to poly-l-lysine-coated slides, and the cell mixture was incubated with the respective primary Abs: rabbit anti-Cx43 (21); monoclonal anti-Cx43 (23); anti-Cx43Hchl, custom-made rabbit Ab raised against the extracellular loop 1 of Cx43, sequence: ESAWGDEQSAFRCNTQQPGC, affinity purified (Genscript Piscataway, NJ, USA); biotin anti-mouse CD3 (145-2C11, BD Pharmingen); or biotin anti-mouse LFA-1 (CD11a I21/7, Leinco Technologies, St Louis, MO). Protein expression was visualized by using the corresponding secondary fluorescence-conjugated Abs: hamster anti-mouse AMCA (Jackson ImmunoResearch, West Grove, PA), streptavidin Alexa Fluor® 488 conjugate (Molecular Probes), goat anti-rabbit DyLight 549 (Pierce, Thermo Scientific Basingstoke, UK), for 1 h. Fluorescently labeled secondary Abs were added alone as negative controls. Cells were analyzed using a Leica inverted TCS SPE (Milton Keynes, UK) confocal microscope (40x, 1.15 NA, oil immersion objective). Thirty-five conjugates/experiment were analyzed in at least three experiments.

MCL-DCs (3×10^5) were co-incubated with 9×10^5 MCL-specific $CD4^+$ T cells (MT56-4) for 1 h. The cell mixture was incubated with an anti-Cx43 Ab (21). Protein expression was

visualized by using the corresponding secondary fluorescence-conjugated Ab Alexa Fluor® 647 goat anti–rabbit (Molecular Probes), which was also added alone as negative control. Cells were analyzed by confocal microscopy (LSM 510; 63x NA 1.4 oil immersion objective; Carl Zeiss).

Cx43-Hchl formation was quantified by using a polyclonal anti-Cx43-Hchl Ab raised to a peptide sequence from the first external loop of Cx43 that recognize Cx43 in an undocked conformation, and is occluded in docked GJs. T cells displaying more than 70% of Cx43-Hchl staining in the quadrant contacting DCs were scored as positive. We also analysed the percentage of cells accumulated at the synapse that were not forming Hchl. To this end a Cx43 monoclonal Ab (mAb) raised against the intracellular loop of Cx43 that recognized total Cx43, as both GJ and hemichannels, was used, and again T cells displaying more than 70% positive staining in the quadrant contacting DCs were scored as positive. We subtracted the number of cells scored as positive for Cx43-Hchl (Figure 4E, dark grey), from the total number of cells scored as positive for Cx43, then obtaining the fraction of cells positive for Cx43, but negative for Hchl (Figure 4E, light grey).

3D reconstructions and projections, and quantitative image analysis

The 3D reconstruction of the confocal image stacks taken from interacting DCs and T cells stained for Cx43, LFA-1 and TCR were accomplished by using Volocity 4.4.0 analysis software (Improvision, Coventry, UK). For 3D reconstructions, ~ 20-25 z sections were collected at 0.3 μm z intervals. The en face view of the immune synapse was obtained by an x-z projection of the 3D image at the cellular interface of the T cell and DC. The ratio of Cx43 fluorescence at the immunological synapse vs. Cx43 fluorescence at the plasma membrane was calculated using ImageJ software (NIH). Statistical analyses were carried out by the non-parametrical Mann-Whitney test. Values of $P < 0.05$ were considered statistically significant.

Co-localization analysis

Manders' colocalization coefficients (24) were calculated at the site of interaction between OT-II T cells and OVA-DCs for TCR/Cx43, CD3/Cx43 and LFA-1/Cx43 using NIH Image J software with the colocalization analysis plugin JACoP. Manders colocalization coefficient calculates the spatial overlap of two proteins, with M1 representing the percentage of Cx43 pixels (red channel) that overlaps pixels in the green channel (CD3 or LFA-1), and conversely for M2. M1 and M2 values range from 0 to 1, with a value of 0 corresponding to non-overlapping images and the latter reflecting 100% co-localization between both images. Manders' coefficients are not influenced by differences in absolute signal intensities in each channel since pixel intensity in a particular channel is normalized to total pixel intensity across the image for that label. Values were reported as mean ± SEM.

Flow cytometry analysis

Flow cytometry experiments were performed as previously described (15). DCs or T cells were pre-treated or not with 40 μM Cx43-sense or Cx43-AS or with 300 μM 1848 Cx43-mimetic peptide for 4 h. $CD11c^+$ cells, corresponding to DCs, were gated and the levels of different markers including Cx43, were analyzed using a double staining. Cells were stained using anti-Cx43 (21); PE-conjugated anti-CD11c (eBioscience); FITC-conjugated anti-CD83, CD40, MHC class I, and MHC class II (BD Pharmingen); PE Cy5.5-conjugated anti-CD4 (eBioscience) Abs. Cells were acquired on a flow cytometer (FACSort; BD Pharmingen) and analyzed using the CellQuest software.

DC-T cell adhesion assay

OT-II T cells and OVA-DCs, pre-treated or not for 4 h with 40 μM Cx43-AS or Cx43-sense (25), were co-incubated for 5 min or 30 min, then fixed and mounted. Images of six random fields from three individual samples per condition were taken with a 4 × 0.1 NA objective on an inverted Axiovert Zeiss LSM microscope. The number of T cells-DCs conjugates was quantified and reported as percentage ± SD.

FRAP experiments

GJIC was quantitatively assessed in living cells by FRAP assay. Gap junctional dye transfer was measured using the AM ester derivative of the fluorescent indicator Calcein (Calcein-AM; Invitrogen). DCs interacting with T cells, pre-treated or not for 4 h with 40 μM murine AS (25) or human Cx43-AS (sequence: GTAATGCGGCAAGAAGAATTGTTTCTGTC); 40 μM Cx43-sense (25); 300 μM Gap20 control peptide; 300 μM 1848 mimetic peptide; or 50 μM 18-β-glycyrrhetinic acid (β-Ga) were collected and loaded with 1 μM calcein-AM in culture medium for 30 min. Once inside the cell, endogenous esterases cleave the lipophilic AM groups, producing fluorescent calcein molecule that is unable to leak out of cells across cell membranes, but is able to pass between cells connected via GJs.

FRAP was performed on a Leica SPUV (Milton Keynes, UK) confocal microscope (40x, 0.8 NA, water immersion objective), using the FRAP function on the Leica confocal software, 1 h after calcein-AM loading. As a control, 1 mM propidium iodide was added to the media to check cell viability during imaging. A region of interest (ROI), either the T cell or the DC, was chosen, and between 12-15 cycles of the 488 nM laser at 12% emission strength were used to photobleach the fluorescence within the ROI. These were the conditions determined for optimal bleaching of the DC-T cell conjugates. The progression of FRAP was followed by continuously acquiring images with a time interval of 5 sec for 2 min of total imaging time. Fluorescence of the mobile fraction was quantified using the Mean ROI function (Image J software). Fluorescence intensities of ROIs were recorded before photobleaching, immediately after photobleaching, and at 5-sec intervals after photobleaching. The percentage of fluorescence recovery was calculated using the equation for determining the mobile fraction (26).

Measurement of Ca^{2+} signals

A Leica SPUV confocal microscope (63x, 1.2 NA, water immersion objective) was used for analysis of Ca^{2+} transients in MCL-specific $CD4^+$ T cells co-cultured with MCL-DCs, as well as in OVA-DCs incubated with OT-II T cells. Cells pre-treated or not for 4 h with 40 μM Cx43-AS, 40 μM Cx43-sense, 300 μM Gap20 control peptide, 300 μM 1848 mimetic peptide, or 50 μM 18-β-glycyrrhetinic acid (β-Ga) were collected and stained with 1 μM Fluo4-AM (Molecular Probes, Invitrogen). The 1848 mimetic peptide and Gap20 control peptide were added back after washing the cells to remove excess probe. The Fluo4-AM fluorescence and bright field were monitored simultaneously by taking frames at 10-s intervals. Intracellular Ca^{2+} signals were reported as total mean fluorescence ± SEM and were quantified as Fluo4 fluorescence at any time point - basal fluorescence obtained by averaging all the frames. The emission intensity was displayed on a pseudocolor scale using the Leica Lite browser software.

IFN-γ ELISPOT assay

MultiScreen plates (MAPN1450; Millipore, Watford, UK) were coated overnight with 2 μg/ml of anti-human IFN-γ capture mAb (1-D1K, Mabtech, Stockholm, Sweden). MCL-DCs and autologous MCL-specific $CD4^+$ T cells were pre-incubated for 4 h in the presence or absence of 300 μM 1848 Cx43-mimetic peptide (sequence (CNTQQPGCENVCY

extracellular loop 1; 95% purity); 300 μM Gap20 control peptide (EIKKFKYGIEEHC cytoplasmic loop; 95% purity) (both from JPT Peptide Technology, Berlin, Germany); 50 μM β-Ga, 40 μM Cx43-AS or vehicle. After this time, 5×10^3 DCs were co-cultured with T cells at a 1:1 ratio for another 4 h. Additionally, non-treated DCs and T cells were co-incubated cells at a 1:1 ratio for another 4 h with T cells and DCs, respectively, which were pre-treated 4 h with the aforementioned drugs or vehicles. IFN-γ spots were counted using an automated counter ELISPOTscan (A.EL.VIS, GmbH, Hannover, Germany).

Statistics

Statistical analysis was done using the Statgraphics-Plus 2.1 software. Differences between treatments were tested by one-way analysis of variance (ANOVA), using Duncan's multiple comparison procedure or the Mann Whitney U test for data sets of multiple comparisons. Results are presented as mean ± SD except where stated. *P*-values < 0.05 were considered statistically significant.

Results

Cx43 accumulation at the T cell stimulatory interface is dependent on the actin cytoskeleton

Beads coated with antibodies directed against CD3 and the co-stimulatory surface receptor CD28 have been widely used to mimic T cell activation by APCs. Cx43 was found to accumulate at the site of contact formed between T cells and beads after stimulation with anti-CD3 and anti-CD28 beads, while a random distribution of Cx43 was observed in T cells incubated with beads coated with an irrelevant antibody (Ab) (Figure 1A). Image analysis confirmed that over 60% of T cells recruited Cx43 following activation with anti-CD3 plus anti-CD28 beads (Figure 1B). In contrast, only 30% of T cells accumulated Cx43 in the presence of anti-CD3 or anti-CD28-coated beads, similar to what was found when using an irrelevant Ab (Figure 1B). Furthermore, accumulation of Cx43 and CD3 was found following T cell engagement, suggesting that Cx43 may be recruited to the stimulatory synapse formed between T cells and APC (Figure 1C).

As recent work has provided evidence for direct targeting of Hchl to cell-cell junctions through a pathway that is dependent on microtubules (27), we investigated whether Cx43 recruitment after TCR engagement was a cytoskeleton-dependent process. The distribution of Cx43 was analyzed by confocal microscopy in human $CD4^+$ T cells, which were incubated with anti-CD3 and anti-CD28 beads in the presence or absence of specific inhibitors of either microtubule or actin polymerization. When microtubule dynamics were inhibited by incubation with taxol or nocodazole, similar accumulation of Cx43 at the site of contact was observed as in the absence of inhibitors (Figure 2A, B and D). In contrast, incubation with either latrunculin A or cytochalasin D (inhibitors of actin polymerization) completely abrogated Cx43 accumulation to the contact area (Figure 2C and D). These results indicate that Cx43 recruitment to the synapse is dependent on the actin cytoskeleton.

Cx43 accumulates at the IS pSMAC in an antigen-specific and time-dependent manner

Cx43 distribution was then investigated by confocal microscopy in conjugates of human dendritic cells (DCs) loaded with a melanoma cell lysate (MCL) and co-cultured with $CD4^+$ T cells that specifically recognize autologous MCL-DCs (Supplementary Figure S1A). Cx43 was found to accumulate to the interface between T cells and MCL-DCs (Figure 3A, arrowhead), but was homogeneously distributed when T cells were incubated with DCs pulsed with the control antigen gp100 (Figure 3A). As the MCL contains a number of unknown antigenic peptides, Cx43 accumulation was further investigated using $CD4^+$ T cells from OT-II mice, which carry a transgenic TCR specifically recognizing the ovalbumin

$(OVA)_{323-339}$ peptide presented in MHC class II. OT-II $CD4^+$ T cells were co-incubated with mature bone marrow-derived DCs (LPS-DCs) or OVA-pulsed mature DCs (OVA-DCs), and synapse formation was visualized by confocal microscopy. Cx43 was found to accumulate at the synapse formed between OT-II T cells and OVA-DCs (Figure 3B, arrowhead), but was almost completely absent when T cells were incubated with LPS-DCs (Figure 3B). Quantification showed that over 60% of OVA-DC and OT-II T cell conjugates concentrated Cx43 at the T cell-DC interface, and a four-fold increase of Cx43 accumulated at the contact area, compared to the plasma membrane (Figure 3C). Similar amounts of Cx43 recruited to the MCL-DCs and MCL-specific T cell interface, and a three-fold increase of Cx43 accumulated at the contact area was observed when using the human model (Figure 3C). In contrast, in the absence of antigen-specific presentation (LPS or gp100), fewer conjugates accumulated Cx43 and reduced Cx43 amounts were found at the site of T cell-DC interaction (Figure 3A-C).

Spatial segregation of accumulated molecules at the IS leads to the formation of cSMAC and pSMAC within the synapse (4). In order to establish to which compartment Cx43 was recruited, the distribution of Cx43 was compared to the distribution of CD3 (cSMAC) and LFA-1 (pSMAC). The Cx43 pool that redistributed to the IS was only partially co-localized with CD3 (Figure 3E and Supplementary Figure S1B), and was found predominantly co-localized with LFA-1 (Figure 3F and Supplementary Figure S1C) in both mouse and human models, indicating a preferential recruitment of Cx43 to the pSMAC ring. This observation of colocalization was calculated by quantification using overlap coefficient according to Manders's automatic threshold determination. Cx43 displayed 63.1% co-localization with LFA-1, against only 35.7% with CD3. The measured co-localization coefficients for Cx43-LFA-1 and LFA-1-Cx43 were statistically higher ($p < 0.05$) compared to the values for Cx43-CD3 and CD3-Cx43 (Figure 3D).

Furthermore, serial optical sections along the z-axis for Cx43, LFA-1 and TCR labeling on OVA-DCs or LPS-DCs contacting OT-II T cells were taken allowing three-dimensional reconstruction and projection on the x-z plane. Figure 3G shows representative en face views illustrating the Cx43 accumulation at the DC-T cell interface. Whereas the TCR clustered in the central zone of a T cell in contact with an OVA-DC, Cx43 was excluded from this area and was found coclustering with LFA-1 at the peripheral zone of contact (Figure 3G). Cx43 accumulation was rare at the site of interaction of conjugates formed between OT-II T cells and LPS-DCs (Figure 3G).

The molecular structure of the IS facilitates antigen recognition and T cell activation. To further investigate whether accumulation of Cx43 at the synapse is antigen-specific, as well as to evaluate dynamic changes in Cx43 recruitment, the distribution of Cx43 was analyzed over time in both mouse and human systems. Accumulation of Cx43 to the contact area of DCs interacting with T cells was quantified and analyzed as previously described (22). Significant higher recruitment of Cx43 to the IS was found in conjugates of OT-II T cells and OVA-DCs (Figure 4A and B; $p < 0.01$ and $p < 0.005$; Supplementary Figure S2A; $p < 0.05$). Maximal accumulation of Cx43 was observed 30-45 min after OT-II T cell/OVA-DC incubation (Figure 4B and C), whereas in the human model statistically significant differences were observed 45 min after MCL-DC and MCL-specific T cell incubation (Supplementary Figure S2A). In contrast, when OT-II T cells were incubated with LPS-DCs, or when MCL-specific T cells were co-cultured with gp-100-DCs, substantially fewer conjugates accumulated Cx43 at the site of interaction (Figure 4A-C; Supplementary Figure S2A). Taken together, these data identify Cx43 as a component of the IS, and suggest that Cx43 recruitment is time-dependent and requires cognate antigen recognition by T cells.

Cx43 accumulates at the IS as Cx-hemichannels

Besides GJs, Cxs can also form stand-alone Hchls; therefore we analyzed whether Hchls may possibly form and accumulate to the IS. To address this, a polyclonal anti-Cx43-Hchl Ab raised to a peptide sequence from the first external loop of Cx43 that recognize Cx43 in an undocked conformation, and is occluded in docked GJs, was used to examine the distribution of Hchls in conjugates of T cells and DCs in both mouse and human systems. This Cx43-Hchl Ab was used in combination with a Cx43 monoclonal Ab (mAb) raised against the intracellular loop of Cx43 (23). Cx43-Hchls formation and synapse accumulation was confirmed in human and mouse DCs-T cells conjugates (Figure 4D; Supplementary Figure S2B). Significant accumulation of Cx43 Hchls was found at the interface of OT-II T cells and OVA-DCs, compared to LPS-DCs, 30 min after conjugate formation (Figure 4E; $p < 0.05$ and $p < 0.01$), and a two-fold increase of Cx43 accumulated at the contact area, compared to the plasma membrane, was observed 2 h after cognate $CD4^+$ T cell–DC interaction in both human and mouse model (Figure 4F, and Supplementary Figure S2C-D). These data provide evidence for Cx43 accumulation at the IS as stand-alone Hchls.

GJs mediate bidirectional communication between DCs and T cells

Bidirectional communication mediated by GJs between cells of the immune system has been previously described (10). The establishment of bidirectional GJIC between DCs and T cells was then monitored by fluorescence recovery after photobleaching (FRAP). OT-II T cells and DCs were loaded with calcein-AM, a fluorescent GJ channel permeant dye, bleached, and the recovery of fluorescence was monitored for 2 min at intervals of 5 sec. Cell viability was verified by propidium iodide exclusion, which was added to the medium and was present throughout the experiment. Cell communication from DCs to T cells, identified as fluorescence recovery, was confirmed 2 min after bleaching OT-II T cells forming conjugates with OVA-DCs (Figure 5A and 5C-D; Supplementary Video 1). Bidirectional transport, in this case from T cells to DCs was observed when OVA-DCs were photobleached and fluorescence recovery monitored (Figure 5B and D; Supplementary Video 2). In contrast, photobleaching of T cells contacting LPS-DCs, or bleaching of LPS-DCs contacting OT-II T cells showed no fluorescence recovery (Figure 5A-D), indicating that this is an antigen-dependent process. Inhibiting Cx43 by means of a Cx43 antisense oligodeoxynucleotide (Cx43-AS ODN) that targets Cx43 expression in T cells and DCs (Supplementary Figure S3A-D), completely blocked fluorescence recovery (Figure 5), confirming that Cx43 is required for functional GJs to form in either direction. In contrast, intercellular communication was not affected when DCs-T cells conjugates were incubated with a Cx43-sense oligo control (Supplementary Figure S3E-F). We also investigated fluorescence recovery after incubation with 18-β glycyrrhetinic acid β-Ga, or the Cx43 mimetic peptide 1848 that blocks docking between adjacent Hchls. Intercellular communication was dramatically reduced after treatment with these inhibitors, while was not affected in cells treated with the Gap20 control peptide (Supplementary Figure S3E-F).

Moreover, FRAP analysis using MCL-specific T cells and DCs confirmed our findings in the human model (Supplementary Figure S3G-H). These results provide support for the role of Cx43 in mediating bidirectional intercellular communication between T cells and DCs at the IS.

Cx43 is required for APC-mediated T cell activation

Binding of TCR to specific MHC-peptide complexes triggers downstream intracellular events and oscillations of intracellular Ca^{2+}, essential for T cell activation (28). Because previous studies have described Cx43 participation in Ca^{2+} influx in various cell types (29, 30), we investigated whether Cx43 was involved in regulating Ca^{2+} signaling in T cells. Calcium signals were monitored over time in T cells co-incubated with MCL-DCs and

loaded with Fluo4-AM. Antigen-specific T cell stimulation resulted in oscillation of intracellular Ca^{2+}, which was impaired when DCs and T cells were pre-incubated and co-cultured in the presence of the different GJ or Cx43 inhibitors (Figure 6A-C). When the Ca^{2+} influx was analyzed in the murine OT-II model system similar findings were obtained (Supplementary Figure S4A-B). No differences were detected in the expression of MHC class I and class II, CD40 and CD83 when DCs were cultured in the presence of Cx43 inhibitors (Figure 6D). Moreover, incubation with the Cx43-AS did not alter the expression of TCR complexes on T cells (Figure 6E). These data indicate that inhibition of GJIC does not affect signals 1 and 2 of T cell activation; therefore the impairment in Ca^{2+} signalling is likely the result of reduced GJ or Hchl activity.

As interactions between opposing GJ Hchls are a form of intercellular adhesion, the contribution of Cx43 to adhesion of T cells and antigen-pulsed DCs was also investigated. Silencing of Cx43 did not substantially alter cell adhesion, and similar numbers of conjugates were formed between untreated, Cx43-AS and Cx43-sense-treated cells (Figure 6F).

To further investigate whether recruitment of Cx43 to the IS contributes to T cell activation, the secretion of IFN-γ was evaluated by ELISPOT after both T cells and DCs were incubated (or not) with β-Ga, the 1848 Cx43-mimetic peptide, Cx43-AS, or their respective controls. T cell activation was significantly reduced after incubation with each of the aforementioned drugs (Figure 6G). In contrast, treatments with control vehicle or irrelevant peptide did not inhibit IFN-γ secretion (Figure 6G). Similarly, when secretion of IFN-γ or IL-2 was analyzed by intracellular FACS following treatment of OT-II T cells stimulated with OVA-pulsed DCs with different GJ or Cx43 inhibitors, T cell activation was found impaired in the murine system as well (Supplementary Figure S4C-E). Furthermore, we evaluated the individual contribution of Cx43 from T cells or DCs to the T cell activation process. When GJ activity was inhibited in DCs only, significant reduction of IFN-γ secretion was detected after pre-incubation with β-Ga or the Cx43-AS ($p < 0.01$ and $p < 0.05$, respectively), but only a slight decrease was obtained after pre-treatment with the 1848-mimetic peptide (Figure 6H). In contrast, T cell activation was more dramatically impaired after pre-incubation of T cells with any of these drugs (Figure 6H; $p < 0.005$). We further investigated IFN-γ secretion in the absence of APCs, following activation with anti-CD3 plus anti-CD28 beads, and after treatment with the 1848 mimetic peptide or a control peptide. IFN-γ secretion was impaired following Cx43-mimetic peptide incubation, but remained unaffected in cells incubated with a control peptide (Supplementary Figure S4F), suggesting a role for Hchls in T cell activation.

Overall, these results suggest a role for GJs and Hchls as coordinators of the DC-T cell signaling machinery that regulates T cell activation.

Discussion

Multiple surface molecules spatially segregated at the IS mediate intercellular communication and activate intracellular signaling pathways, resulting in T cell activation and proliferation. Antigen-dependent T cell activation is a cell-cell contact-dependent process, suggesting that mediators of intercellular communication are directly involved. In this study we have used a combination of experimental approaches to show that Cx43 accumulates at the IS during specific cognate DC-T cell interaction as both GJs and stand-alone Hchls. Redistribution of Cx43 to the IS was antigen-specific and time-dependent, with maximal accumulation occurring as early as 30 min after DC-T cell conjugate formation, at which time a mature IS has been formed (31). The mature immunological synapse is characterized by a prototypical cSMAC with accumulated MHC:peptide and TCR, among

others, surrounded by a pSMAC enriched in molecules such as ICAM-1 and LFA-1 (3, 4). Here we found Cx43 accumulated at the pSMAC in T cells and colocalized with LFA-1, which is essential for adhesion and signaling within the IS. Although interactions between opposing Hchls are a form of intercellular adhesion and both adhesion proteins and GJs act in a coordinated fashion to join cells together and allow communication between them (32), silencing of Cx43 did not affect T cell-DC cell adhesion within the synapse.

Cell-surface molecules from all over the T cell membrane are transported to the IS through a mechanism involving the cell cytoskeleton and motor proteins (33). Here we show that Cx43 recruitment to the synapse required an intact actin cytoskeleton, as inhibitors of actin polymerization abolished Cx43 accumulation. Although targeting of Cx-Hchls to the plasma membrane, which is essential for GJ formation, involves the microtubule network (27), in our hands inhibition of microtubules did not affect the recruitment of Cx43 to the synapse. Therefore, the Cx43 pool relocated to the IS is not likely to be newly synthesized Cx43, but Cx43 already allocated in the plasma membrane that redistributed to the synapse.

The specific involvement of Cx43 GJ-channels in mediating bidirectional communication between DCs and T cells at the IS was demonstrated, and the use of either a GJ drug-inhibitor, a specific mimetic-peptide, or gene-targeting by means of a Cx43-AS ODN resulted in blockage of intercellular communication between these cells. Intercellular communication has been previously described between regulatory and effector T lymphocytes (14), follicular DCs and B cells in lymph nodes (34), lymphocytes and endothelial cells (18) and between T cells and B cells (19). Moreover, it was recently shown that GJs mediate communication between macrophages and T lymphocytes, in particular the Th1 cell subset (35), as well as unidirectional communication from DCs to T cells (16), which further reinforces our observations. Cx43 accumulation at the IS and Cx43-mediated T cell-DC functional coupling indicate a direct correlation between both processes, and implicates this protein in mediating signals between these two cell subtypes. The nature of the intracellular signals exchanged through GJs at the synapse is presently unknown, and further studies are required to identify the molecules that travel through GJs formed between DCs and T cells. Whereas GJs form channels that allow direct intercellular communication between adjacent cells, Hchls represent “pores” formed by a characteristic hexameric assembly of Cx subunits, and mediate communication between cells and their extracellular environment. Even though it has been described that under physiological conditions Hchls composed of Cx43 have a low open probability (29), different reports have demonstrated that they are able to release physiologically relevant quantities of signaling molecules to the extracellular milieu, including NAD^+ and glutamate, and to mediate ATP release that induces intercellular Ca^{2+} signals (36-38).

Activation of T lymphocytes via stimulation of the TCR complex is marked by a rapid and sustained increase of intracellular Ca^{2+}, which is required for gene transcription, cellular proliferation, and differentiation (39). A sustained Ca^{2+} signal for many hours is also necessary to stimulate nuclear factor of activated T cells (NFAT), a transcription factor that regulates the expression of various cytokine genes, including IL-2 (39, 40). Different studies have described Cx43 participating in Ca^{2+} influx in various cell types (41). In this work, we presented evidence supporting the participation of Cx43 in regulating Ca^{2+} oscillations in the IS. We demonstrated that specific blockade of Cx43 prevents the sustained rise of intracellular Ca^{2+} that was seen in T cells forming conjugates with antigen-pulsed DCs, in both murine and human models. Cell adhesion is important for the Ca^{2+} flux that is required for T cell activation, but Cx43 gene targeting did not affect adhesion between T cells and DCs, as Cx43 inhibition did not influence the formation of DC-T cell clusters. This result indicates that the reduced Ca^{2+} response seen was the result of inhibition of GJIC rather than of Cx43-mediated cell adhesion.

The increase in intracellular Ca^{2+} is an obligatory step in the cascade of signals that finally results in T cell proliferation (42).. Moreover, a role for GJs in T cell activation was recently described, and inhibition of GJIC was responsible for reduced IL-2 secretion and cell proliferation (16). The impaired Ca^{2+} signals we observed as a result of blocking GJs and Cx43 are likely to account for the reduced lymphocyte activation seen after inhibiting GJIC, suggesting that Ca^{2+} signals regulated by GJs may possibly be one the mechanisms controlling T cell activation. Hchls have also been implicated in controlling sustained proliferation of activated $CD4^+$ T cells (43), and here we showed that beside GJs, Cx43 also accumulate at the IS as Hchls, which can regulate Ca^{2+} signaling (44) and mediate ATP release through a mechanism dependent on intracellular Ca^{2+} mobilization (30). Whereas selective blockers for Hchls are not yet known, treatments with a Cx43-mimetic peptide proved Cx43 to be important in regulating Ca^{2+} oscillations. Even though mimetic peptides inhibit intercellular coupling and prevent assembly of newly formed functional GJ channels, some functionality for Cx-Hchls cannot be excluded as mimetic peptides can also bind to Cx-Hchls, block Hchl docking and restrict ATP release (45).

Our findings also show that Cx43 participates in the regulation of IFN-γ secretion as both gene-targeting of Cx43 and blockade of Cx43-GJ function substantially diminished IFN-γ secretion by primed T cells. In addition, cytokines can positively regulate the surface expression of Cxs and GJIC in cells of the immune system (17), suggesting the existence of a positive feedback regulation by cytokines, such as IFN-γ, which can stimulate opening of GJ channels and Cx43 upregulation (13). Such a mechanism may contribute to sustained communication between T cell and APCs, allowing optimal T cell activation. Although we have shown that GJIC is important for T cell activation, we cannot exclude a possible contribution for Hchls to this process. The fact that a Cx43-mimetic peptide has also affected IFN-γ secretion by T cells following incubation with anti-CD3 and anti-CD28 beads suggests that these structures are also involved in T cell activation. This role additionally correlates with our findings of Hchl accumulation at the site of contact between T cells and DCs. As targeting of Cx43 protein expression or the use of a specific Cx43-mimetic peptide block both GJ and Hchl, further studies using Cx43 mutants may provide useful tools to discern the contribution of Hchl to antigen-specific T cell activation.

In summary, this work identifies Cx43 as a key component of the IS and provides evidence of a role for GJ and Hchl in T cell activation, opening new questions regarding the involvement of these structures in the regulation and synchronization of immunological processes.

Supplementary Material

Refer to Web version on PubMed Central for supplementary material.

Acknowledgments

We are particurlarly grateful to L. Saragoni and C. Thrasivoulou for confocal support and M. Briones for technical help. The authors want to thank J. Cook and P. Cormie for critical reading of the manuscript and useful discussions.

This work was funded by grants from the Millennium Institute of Immunology and Immunotherapy (P04/030-F, FSO), grants from the Chilean National Fund for Scientific and Technological Development (FONDECYT 1090238, FSO; and FONDECYT 3070036, AMN), the European Union (Marie Curie Intraeuropean fellowship 040855, GB) and the Wellcome Trust (057965/Z/99/B, AJT; and 090233/Z/09/Z, GB and AJT).

References

1. Babbitt BP, Allen PM, Matsueda G, Haber E, Unanue ER. Binding of immunogenic peptides to Ia histocompatibility molecules. Nature. 1985; 317:359–361. [PubMed: 3876513]

2. Hedrick SM, Nielsen EA, Kavaler J, Cohen DI, Davis MM. Sequence relationships between putative T-cell receptor polypeptides and immunoglobulins. Nature. 1984; 308:153–158. [PubMed: 6546606]
3. Grakoui A, Bromley SK, Sumen C, Davis MM, Shaw AS, Allen PM, Dustin ML. The immunological synapse: a molecular machine controlling T cell activation. Science. 1999; 285:221–227. [PubMed: 10398592]
4. Monks CR, Freiberg BA, Kupfer H, Sciaky N, Kupfer A. Three-dimensional segregation of supramolecular activation clusters in T cells. Nature. 1998; 395:82–86. [PubMed: 9738502]
5. Trautmann A, Valitutti S. The diversity of immunological synapses. Curr Opin Immunol. 2003; 15:249–254. [PubMed: 12787748]
6. Loewenstein WR. Junctional intercellular communication: the cell-to-cell membrane channel. Physiol Rev. 1981; 61:829–913. [PubMed: 6270711]
7. Saez JC, Connor JA, Spray DC, Bennett MV. Hepatocyte gap junctions are permeable to the second messenger, inositol 1,4,5-trisphosphate, and to calcium ions. Proc Natl Acad Sci U S A. 1989; 86:2708–2712. [PubMed: 2784857]
8. Goodenough DA. The structure of cell membranes involved in intercellular communication. Am J Clin Pathol. 1975; 63:636–645. [PubMed: 1130322]
9. Musil LS, Goodenough DA. Biochemical analysis of connexin43 intracellular transport, phosphorylation, and assembly into gap junctional plaques. J Cell Biol. 1991; 115:1357–1374. [PubMed: 1659577]
10. Oviedo-Orta E, Gasque P, Evans WH. Immunoglobulin and cytokine expression in mixed lymphocyte cultures is reduced by disruption of gap junction intercellular communication. Faseb J. 2001; 15:768–774. [PubMed: 11259395]
11. Zahler S, Hoffmann A, Gloe T, Pohl U. Gap-junctional coupling between neutrophils and endothelial cells: a novel modulator of transendothelial migration. J Leukoc Biol. 2003; 73:118–126. [PubMed: 12525569]
12. Neijssen J, Herberts C, Drijfhout JW, Reits E, Janssen L, Neefjes J. Cross-presentation by intercellular peptide transfer through gap junctions. Nature. 2005; 434:83–88. [PubMed: 15744304]
13. Matsue H, Yao J, Matsue K, Nagasaka A, Sugiyama H, Aoki R, Kitamura M, Shimada S. Gap junction-mediated intercellular communication between dendritic cells (DCs) is required for effective activation of DCs. J Immunol. 2006; 176:181–190. [PubMed: 16365409]
14. Bopp T, Becker C, Klein M, Klein-Hessling S, Palmetshofer A, Serfling E, Heib V, Becker M, Kubach J, Schmitt S, Stoll S, Schild H, Staege MS, Stassen M, Jonuleit H, Schmitt E. Cyclic adenosine monophosphate is a key component of regulatory T cell-mediated suppression. J Exp Med. 2007; 204:1303–1310. [PubMed: 17502663]
15. Mendoza-Naranjo A, Saez PJ, Johansson CC, Ramirez M, Mandakovic D, Pereda C, Lopez MN, Kiessling R, Saez JC, Salazar-Onfray F. Functional gap junctions facilitate melanoma antigen transfer and cross-presentation between human dendritic cells. J Immunol. 2007; 178:6949–6957. [PubMed: 17513744]
16. Elgueta R, Tobar JA, Shoji KF, De Calisto J, Kalergis AM, Bono MR, Rosemblatt M, Saez JC. Gap junctions at the dendritic cell-T cell interface are key elements for antigen-dependent T cell activation. J Immunol. 2009; 183:277–284. [PubMed: 19542439]
17. Eugenin EA, Branes MC, Berman JW, Saez JC. TNF-alpha plus IFN-gamma induce connexin43 expression and formation of gap junctions between human monocytes/macrophages that enhance physiological responses. J Immunol. 2003; 170:1320–1328. [PubMed: 12538692]
18. Jara PI, Boric MP, Saez JC. Leukocytes express connexin 43 after activation with lipopolysaccharide and appear to form gap junctions with endothelial cells after ischemia-reperfusion. Proc Natl Acad Sci U S A. 1995; 92:7011–7015. [PubMed: 7624360]
19. Oviedo-Orta E, Hoy T, Evans WH. Intercellular communication in the immune system: differential expression of connexin40 and 43, and perturbation of gap junction channel functions in peripheral blood and tonsil human lymphocyte subpopulations. Immunology. 2000; 99:578–590. [PubMed: 10792506]

20. López MN, Pereda C, Segal G, Muñoz L, Aguilera R, González FE, Escobar A, Ginesta A, Reyes D, Gonzalez R, mendoza-Naranjo A, Larrondo M, Compan A, Ferrada C, Salazar-Onfray F. Prolonged survival of dendritic cell–vaccinated melanoma patients correlates with tumor-specific delayed type IV hypersensitivity response and reduction of tumor growth factor β-expressing T cells. J Clin Oncol. 2009; 27:945–52. [PubMed: 19139436]
21. Retamal MA, Cortes CJ, Reuss L, Bennett MV, Saez JC. S-nitrosylation and permeation through connexin 43 hemichannels in astrocytes: induction by oxidant stress and reversal by reducing agents. Proc Natl Acad Sci U S A. 2006; 103:4475–4480. [PubMed: 16537412]
22. Batista A, Millan J, Mittelbrunn M, Sanchez-Madrid F, Alonso MA. Recruitment of transferrin receptor to immunological synapse in response to TCR engagement. J Immunol. 2004; 172:6709–6714. [PubMed: 15153487]
23. Wright CS, Becker DL, Lin JS, Warner AE, Hardy K. Stage-specific and differential expression of gap junctions in the mouse ovary: connexin-specific roles in follicular regulation. Reproduction. 2001; 121:77–88. [PubMed: 11226030]
24. Costes SV, Daelemans D, Cho EH, Dobbin Z, Pavlakis G, Lockett S. Automatic and quantitative measurement of protein-protein colocalization in live cells. Biophysical journal. 2004; 86:3993–4003. [PubMed: 15189895]
25. Qiu C, Coutinho P, Frank S, Franke S, Law LY, Martin P, Green CR, Becker DL. Targeting connexin43 expression accelerates the rate of wound repair. Curr Biol. 2003; 13:1697–1703. [PubMed: 14521835]
26. Lippincott-Schwartz J, Snapp E, Kenworthy A. Studying protein dynamics in living cells. Nat Rev Mol Cell Biol. 2001; 2:444–456. [PubMed: 11389468]
27. Shaw RM, Fay AJ, Puthenveedu MA, von Zastrow M, Jan YN, Jan LY. Microtubule plus-end-tracking proteins target gap junctions directly from the cell interior to adherens junctions. Cell. 2007; 128:547–560. [PubMed: 17289573]
28. Dolmetsch RE, Lewis RS. Signaling between intracellular Ca2+ stores and depletion-activated Ca2+ channels generates [Ca2+]i oscillations in T lymphocytes. J Gen Physiol. 1994; 103:365–388. [PubMed: 8195779]
29. Contreras JE, Saez JC, Bukauskas FF, Bennett MV. Gating and regulation of connexin 43 (Cx43) hemichannels. Proc Natl Acad Sci U S A. 2003; 100:11388–11393. [PubMed: 13130072]
30. Cotrina ML, Lin JH, Alves-Rodrigues A, Liu S, Li J, Azmi-Ghadimi H, Kang J, Naus CC, Nedergaard M. Connexins regulate calcium signaling by controlling ATP release. Proc Natl Acad Sci U S A. 1998; 95:15735–15740. [PubMed: 9861039]
31. Lee KH, Holdorf AD, Dustin ML, Chan AC, Allen PM, Shaw AS. T cell receptor signaling precedes immunological synapse formation. Science. 2002; 295:1539–1542. [PubMed: 11859198]
32. Hillis GS, Duthie LA, Brown PA, Simpson JG, MacLeod AM, Haites NE. Upregulation and co-localization of connexin43 and cellular adhesion molecules in inflammatory renal disease. J Pathol. 1997; 182:373–379. [PubMed: 9306956]
33. Wulfing C, Davis MM. A receptor/cytoskeletal movement triggered by costimulation during T cell activation. Science. 1998; 282:2266–2269. [PubMed: 9856952]
34. Krenacs T, van Dartel M, Lindhout E, Rosendaal M. Direct cell/cell communication in the lymphoid germinal center: connexin43 gap junctions functionally couple follicular dendritic cells to each other and to B lymphocytes. Eur J Immunol. 1997; 27:1489–1497. [PubMed: 9209502]
35. Bermudez-Fajardo A, Yliharsila M, Evans WH, Newby AC, Oviedo-Orta E. CD4+ T lymphocyte subsets express connexin 43 and establish gap junction channel communication with macrophages in vitro. J Leukoc Biol. 2007; 82:608–612. [PubMed: 17596336]
36. Bruzzone S, Guida L, Zocchi E, Franco L, De Flora A. Connexin 43 hemi channels mediate Ca2+-regulated transmembrane NAD+ fluxes in intact cells. FASEB J. 2001; 15:10–12. [PubMed: 11099492]
37. Stout CE, Costantin JL, Naus CC, Charles AC. Intercellular calcium signaling in astrocytes via ATP release through connexin hemichannels. J Biol Chem. 2002; 277:10482–10488. [PubMed: 11790776]
38. Ye ZC, Wyeth MS, Baltan-Tekkok S, Ransom BR. Functional hemichannels in astrocytes: a novel mechanism of glutamate release. J Neurosci. 2003; 23:3588–3596. [PubMed: 12736329]

39. Lewis RS. Calcium signaling mechanisms in T lymphocytes. Annu Rev Immunol. 2001; 19:497–521. [PubMed: 11244045]
40. Crabtree GR. Generic signals and specific outcomes: signaling through Ca2+, calcineurin, and NF-AT. Cell. 1999; 96:611–614. [PubMed: 10089876]
41. Lin GC, Rurangirwa JK, Koval M, Steinberg TH. Gap junctional communication modulates agonist-induced calcium oscillations in transfected HeLa cells. J Cell Sci. 2004; 117:881–887. [PubMed: 14762115]
42. Jensen BS, Odum N, Jorgensen NK, Christophersen P, Olesen SP. Inhibition of T cell proliferation by selective block of Ca(2+)-activated K(+) channels. Proc Natl Acad Sci U S A. 1999; 96:10917–10921. [PubMed: 10485926]
43. Oviedo-Orta E, Perreau M, Evans WH, Potolicchio I. Control of the proliferation of activated CD4+ T cells by connexins. J Leukoc Biol. 2010; 88:79–86. [PubMed: 20233983]
44. Quist AP, Rhee SK, Lin H, Lal R. Physiological role of gap-junctional hemichannels. Extracellular calcium-dependent isosmotic volume regulation. J Cell Biol. 2000; 148:1063–1074. [PubMed: 10704454]
45. Evans WH, De Vuyst E, Leybaert L. The gap junction cellular internet: connexin hemichannels enter the signalling limelight. Biochem J. 2006; 397:1–14. [PubMed: 16761954]

Europe PMC Funders Author Manuscripts

Europe PMC Funders Author Manuscripts

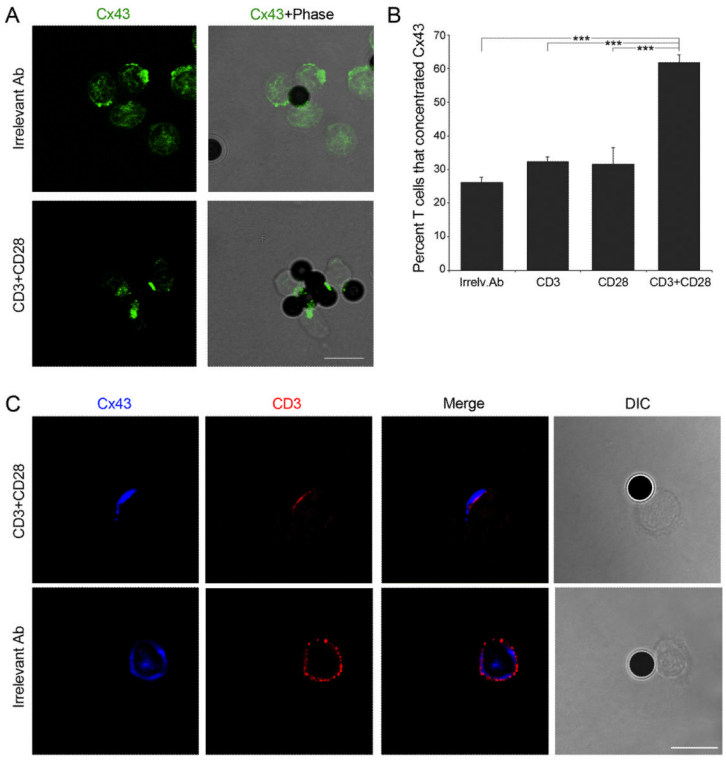

Figure 1. Co-stimulatory signals induce Cx43 accumulation at the contact site

(**A**) Cx43 distribution was analyzed in T cells stimulated with magnetic beads coated with anti-CD3 and anti-CD28, or with an irrelevant Ab. Scale bar = 10 μm. (**B**) The number of T cells that accumulate Cx43 at the site contacting the beads was quantified under the different conditions studied. Values are expressed as the percentage of cells that polarized Cx43 to the contact site, relative to the total number of cells examined. Each plotted point represents mean ± SD of four independent experiments. Differences are indicated by P-values (***, $p < 0.005$). (**C**) The distribution of Cx43 and CD3 was analyzed by confocal microscopy in T cells stimulated with magnetic beads coated with an irrelevant Ab or with anti-CD3 plus anti-CD28. Images are representative of three independent experiments. Scale bar = 10 μm.

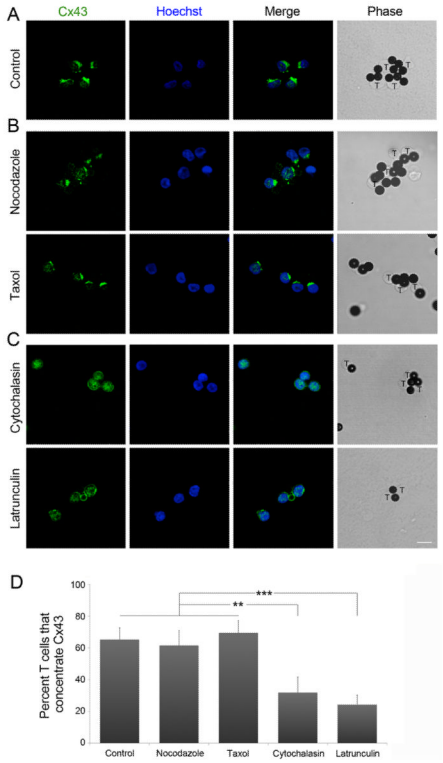

Figure 2. Recruitment of Cx43 is an actin-dependent process

PBLs were incubated for 30 min in the presence, or (**A**) absence, of (**B**) taxol or nocodazole, or (**C**) cytochalasin D or latrunculin A, before incubation with CD3 and CD28-coated beads. Cx43 and Hoechst staining were analyzed by confocal microscopy. The inducible capping of Cx43 to the contact area was impaired in the presence of the inhibitors of actin polymerization. Scale bar = 10 μm. (**D**) The number of T cells that accumulate Cx43 at the site contacting the beads was quantified under the different conditions studied. Values are expressed as the percentage of cells that recruit Cx43 to the IS, relative to the total number of cells examined. Differences are indicated by *P*-values (**, $p < 0.01$; ***, $p < 0.005$).

Europe PMC Funders Author Manuscripts

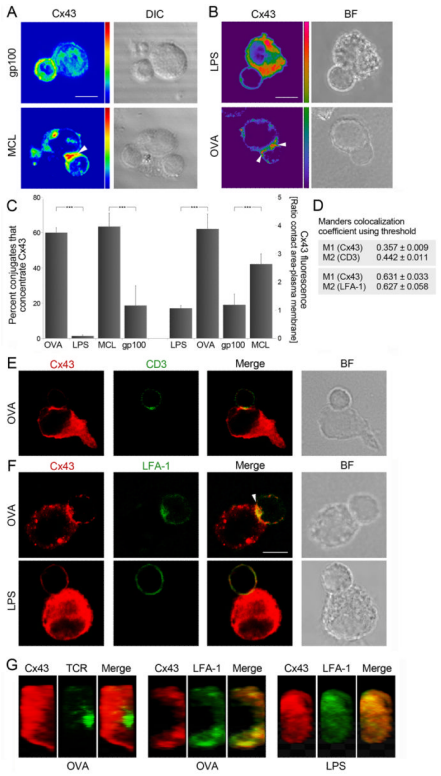

Figure 3. Cx43 is recruited to the IS and accumulates preferentially in the pSMAC between T cells and DC

Cx43 accumulates at the site of interaction of (**A**) MCL-DCs and MCL-specific T cells (arrowheads), and (**B**) OVA-DCs and OT-II CD4$^+$ T cells (arrowheads); but distributes homogeneously in T cells incubated with gp100-DCs and LPS-DCs (**A** and **B**, respectively). Scale bar = 5 μm. (**C**) The number of T cells that accumulate Cx43 at the site of contact, and the ratio of Cx43 fluorescence accumulated at the contact area vs. at the plasma membrane were quantified. Values are expressed as mean ± SD of three independent experiments. Differences are indicated by *P*-values (***, $p < 0.005$). (**D**) The colocalization coefficients for Cx43 (M1 channel) and for CD3 or LFA-1 (M2 channel) were calculated using Manders' automatic threshold determination. Manders' coefficients range from 0 (no overlap) to 1 (complete overlap). Values appear indicated as mean ± SEM. Cells were co-stained for Cx43 and: (**E**) CD3 and (**F**) LFA-1 distribution was evaluated by confocal microscopy in conjugates of OVA-DCs (or LPS-DCs, in **F**) and OT-II T cells. Cx43 was found partially co-localizing with CD3 (**E**) and was mainly accumulated in the pSMAC within the IS (**F**, arrowhead). Scale bar = 5 μm. (**G**) En face views illustrating the Cx43 accumulation at the DC-T cell interface. Cx43 was preferentially concentrated in the peripheral (pSMAC) area of the immunological synapse.

Europe PMC Funders Author Manuscripts

Europe PMC Funders Author Manuscripts

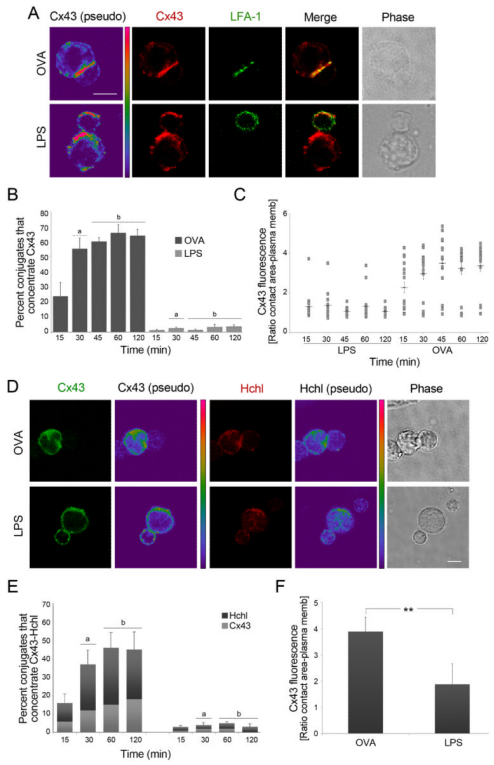

Figure 4. Cx43 and Cx43-Hchls accumulate at the IS in a time-dependent and Ag-specific way

(**A**) Representative images of Cx43 and LFA-1 distribution after incubation of OVA-DCs or LPS-DCs with OT-II T cells are shown. Scale bar = 5 μm. (**B**) Cx43 accumulation at the IS was evaluated at different time points based on positive co–staining of Cx43 and LFA-1 in OVA-DCs or LPS-DCs co-cultured with OT-II T cells. Each plotted point represents mean ± SD of three independent experiments (a: $p < 0.01$ and b: $p < 0.005$). (**C**) Cx43 distribution to the synapse was measured as ratio of Cx43 accumulated at the contact site vs. at the plasma membrane, and was evaluated at different time points. Cx43 accumulation was significantly higher in T cells co-cultured with OVA-DCs vs. LPS-DCs (30 min: $p < 0.01$; and 45, 60 and 120 min: $p < 0.005$). Values are expressed as mean ± SEM; n = 3. (**D**) Hchls and Cx43 accumulates at the site of interaction of OVA-DCs and OT-II $CD4^+$ T cells, but distributes randomly in T cells incubated with LPS-DCs. Scale bar = 5 μm. (**E**) The percentage of cells that accumulated Hchls (dark grey) and Cx43 (light grey) at the synapse was assessed. Values are reported as mean ± SEM (a: $p < 0.05$ and b: $p < 0.01$). (**F**) The ratio of Cx43 fluorescence accumulated at the contact area vs. at the plasma membrane was quantified 2 h after DC-T cells conjugates formation. Values are expressed as mean ± SD of three independent experiments. Differences are indicated by *P*-values (**, $p < 0.01$).

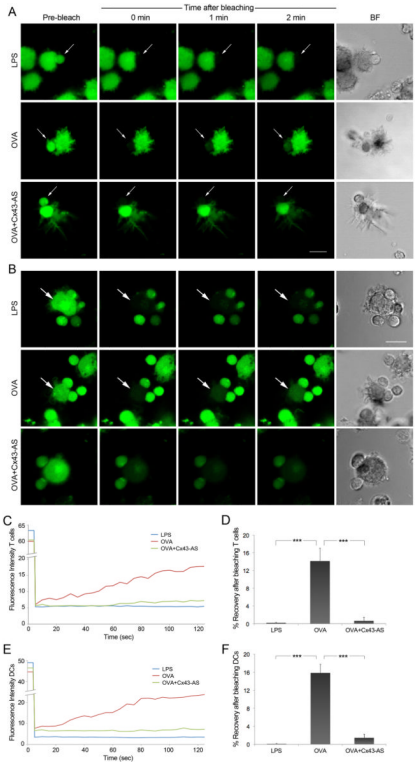

Figure 5. DCs and T cells communicate through functional GJs

(**A**) FRAP experiments were carried out in conjugated formed between LPS-DCs or OVA-DCs and OT-II T cells. Co-cultures of OVA-DCs and T cells pre-treated 4 h with a Cx43-AS were also analyzed. After loading both cell populations with calcein-AM (green), T cells were bleached and the fluorescence recovery was monitored over a period of 2 min. Representative images of fluorescence restoration (or not) and bright field (BF) images are shown. Arrows indicate the target cell before and after photobleaching. Scale bar = 10 μm. (**B**) OVA-DCs or LPS-DCs, and OT-II T cells were loading with calcein-AM (green), DCs were bleached and the fluorescence recovery in the photobleached region was monitored over a period of 2 min. Representative images of fluorescence restoration (or not) and bright field images corresponding to the same fields are shown. Arrows indicate the target cell before and after photobleaching. Scale bar = 10 μm. (**C** and **E**) Representative fluorescence recovery curves for T cells and DCs, respectively illustrating the kinetic profile for each condition are shown. Recovery was confirmed only between OVA-DCs and OT-II T cells conjugates and was negative for the other conditions. (**D** and **F**) Data was analyzed to show the incidence of dye coupling after photobleaching of T cells or DCs, respectively. Mean values were expressed as percentage ± SEM (*, $p < 0.05$); n = 3.

Europe PMC Funders Author Manuscripts

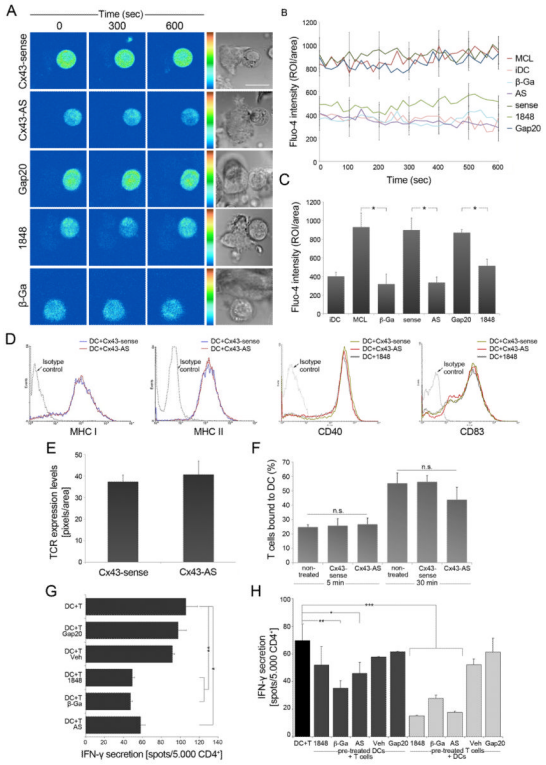

Figure 6. Cx43 contributes to T cell activation by DC

(**A**) Ca^{2+} signalling was analyzed using Fluo4-AM by sequential confocal images of MCL-specific T cells co-cultured with autologous MCL-DCs and treated with different GJs or Cx43 inhibitors and their respective controls. Phase-contrast images corresponding to the same fields are shown. Scale bar = 5 μm. (**B**) Time course showing changes of intracellular Ca^{2+} signalling in T cells contacting DCs, under different conditions. Ca^{2+} signals are shown as total mean fluorescence ± SEM. (**C**) Overall mean of Fluo4-AM fluorescence over the time ± SEM for each condition (*, $p < 0.05$); n = 3. (**D** and **E**) Treatments with a Cx43-AS or with the 1848 Cx43-mimetic peptide did not affect the expression of MHC class I and class II, CD40, CD83 and TCR. (**F**) Cell adhesion was evaluated in conjugates of OVA-DCs and OT-II T cells treated or not with a Cx43-sense or Cx43 AS. Cx43 gene targeting did not affect conjugate formation 5 min and 30 min after DCs-T cells co-incubation. Each bar represents percentage ± SD of four independent experiments. (**G**) IFN-γ secretion was assessed by ELISPOT assay in MCL-specific $CD4^+$ T cells co-incubated with MCL-DCs, plus a non-specific GJ blocker (β-Ga), Cx43-AS or 1848 Cx43-mimetic peptide. Inhibition of GJIC significantly reduced the secretion of IFN-γ by $CD4^+$ T cells. Data were expressed as the mean of spots / 5×10^3 effector cells ± SD (**, $p < 0.01$; *, $p < 0.05$), n = 2, performed in triplicate). (**H**) MCL-DCs or MCL-specific T cells were independently pre-treated with β-Ga, 1848-mimetic peptide, Cx43-AS or their respective controls, and then incubated with non-treated T cells (dark grey) or DCs (light grey), respectively. Control, non-treated T cells and DCs (black) were also evaluated. Graphic represents IFN-γ secretion reported as the mean of spots / 5×10^3 $CD4^+$ T cells ± SD (*, $p < 0.05$; **, $p < 0.01$ and ***, $p < 0.005$) n = 2, performed in triplicate.

Europe PMC Funders Author Manuscripts